Thermophysical and Thermodynamic Properties of 1-Butyl-3-methylimidazolium Tetrafluoroborate and 1-Butyl-3-methylimidazolium Hexafluorophosphate over an Extended Pressure Range

Ricardo Gomes de Azevedo,[†] José M. S. S. Esperança,[†] Vesna Najdanovic-Visak,[†] Zoran P. Visak,[†] Henrique J. R. Guedes,[‡] Manuel Nunes da Ponte,[†] and Luís P. N. Rebelo*[,†]

Instituto de Tecnologia Química e Biológica, ITQB 2, Universidade Nova de Lisboa, Av. República, Apartado 127, 2780-901 Oeiras, Portugal, and REQUIMTE, Departamento de Química, Faculdade de Ciências e Tecnologia, Universidade Nova de Lisboa, 2829-516 Caparica, Portugal

The current study focuses on 1-butyl-3-methylimidazolium tetrafluoroborate, [bmim][BF_4], and 1-butyl-3-methylimidazolium hexafluorophosphate, [bmim][PF_6]. The objective is to study the influence of pressure as well as that of the anion on several properties of this type of ionic liquid. The speed of sound and densities in pure ionic liquids (ILs) as a function of temperature and pressure have been determined. Several other thermodynamic properties such as compressibilities, expansivities, and heat capacities have been obtained. To the best of our knowledge, this research comprises both the first speed of sound data and the first evaluation of heat capacities at high pressures for ILs. Speed of sound measurements have been carried out in broad ranges of temperature ($283 < T/\mathrm{K} < 323$) and pressure ($0.1 < p/\mathrm{MPa} < 150$), sometimes inside the metastable liquid region using a nonintrusive microcell. The $T-P$ melting line of [bmim][PF_6] has also been determined by an acoustic method. Density measurements have been performed for broad ranges of temperature ($298 < T/\mathrm{K} < 333$) and pressure ($0.1 < p/\mathrm{MPa} < 60$) using a vibrating tube densimeter. The pressure dependence of the heat capacities, which is generally mild, is found to be highly dependent on the curvature of the temperature dependence of the density.

Introduction

Despite the fact that hexafluorophosphate, $[PF_6]^-$, and tetrafluoroborate, $[BF_4]^-$, based ILs can undergo hydrolysis producing HF in contact with water[1] (mainly at high temperatures[2]), they are historically the most important and most commonly investigated. We have thus chosen these anions coupled with the much studied cation 1-butyl 3-methylimidazolium for our initial speed of sound studies.

Despite the increasing attention that room-temperature ionic liquids (RTILs) have recently received with respect to their thermophysical and thermodynamic properties, overall information is still scarce. Examples of very recent reviews and systematic studies can be found, for instance, in references 3−6 and references therein.

The speed of sound, u, is a property that can be experimentally determined with great precision over a broad range of temperature and pressure. Because u can be related to the first pressure partial derivative of density, accurate speed of sound data can be used to enhance the development of equations of state. Furthermore, it is a very useful source of information for computing values of other thermodynamic properties that are difficult to obtain at extreme experimental conditions, such as calorimetric data at high pressures. One possible method for deriving a wealth of thermodynamic properties consists of the measurement of the whole (p, ρ, T) and (p, u, T) surfaces to obtain by differentiation the derived properties of the investigated compound. This method has proven useful, for instance, in the calculation of derived properties of protonated and deuterated acetone.[7,8] However, commonly accepted as a more reliable method for deriving thermodynamic properties from speed of sound data is that which allows, by integration, the calculation of (p, ρ, T) and (p, C_p, T) surfaces from merely one isobar of both density and isobaric heat capacity.[9−12] This method allows one to calculate other thermophysical properties such as isentropic (κ_S) and isothermal (κ_T) compressibilities, isobaric thermal expansivities (α_p), isobaric (C_p) and isochoric (C_v) heat capacities, and thermal pressure coefficients (γ_v) over the entire range of pressure of the speed of sound measurements. Whenever available, these values are compared with literature data obtained via other methods.

Experimental Section

Acoustic Cell and Densimeter. Measurements of the speed of sound were performed in the temperature range of $283 < T/\mathrm{K} < 323$ and pressure range of $0.1 < P/\mathrm{MPa} < 150$. The speed of propagation of sound waves in liquids was determined using a nonintrusive method at an operational frequency of 0.5 MHz. We used the same experimental setup as previously described in great detail elsewhere.[7] Pressure was measured using an Omega pressure transducer, which was calibrated against a high-accuracy Heise gauge. The pressure precision and accuracy are better than ±0.05%. The acoustic cell was placed in a Hart Scientific calibration bath (stability ±0.001 K), and temperature was measured by a four-wire platinum resistance thermometer (PRT) coupled to a Keithley digital multimeter (model DMM 199). The PRT was previously

* To whom correspondence should be addressed. E-mail: luis.rebelo@itqb.unl.pt. Phone: +351-21 4469 441. Fax: +351−21 4411 277.
† Instituto de Tecnologia Química e Biológica.
‡ REQUIMTE.

10.1021/je049534w CCC: $30.25
Published on Web 04/21/2005

calibrated, thus allowing temperature measurements on the ITS-90 scale with an estimated uncertainty of better than ±0.01 K. Typically, the uncertainty and repeatability of the speed of sound measurements are ±0.2% and ±0.05%, respectively. Likewise, densities were measured using an Anton Paar DMA 512P densimeter[7] in the temperature range of 298 K to 333 K and the pressure range of 0.1 MPa to 60 MPa. The density overall uncertainty is estimated to be better than 0.02%. It should be noted that this value might increase slightly if one considers possible viscosity corrections.[13] These corrections rely on both the existence of viscosity data[5] and properly evaluated equations for the correlation between viscosity and signal damping. As for the first, to date there are no viscosity data for these ILs at pressures different from atmospheric. In the case of the latter, different corrections have been proposed[13] that basically depend on the instrument model and viscosity range. These issues are still under debate. In light of the above-mentioned caveats, we have not performed any viscosity corrections. Therefore, all of the results of the subsequent derived properties and their discussion are based on raw density data. Nonetheless, at atmospheric pressure, one should expect a downward density shift in the low-temperature range between 0.05% and 0.06% and 0.03% and 0.04% for [bmim][PF_6] and [bmim][BF_4], respectively, decreasing to about 0.02% for both ILs in the high-temperature range.

Chemicals. [bmim][PF_6] was synthesized and purified at the QUILL Centre, Belfast, according to procedures found elsewhere.[14,15] It was washed several times with water to decrease the chloride content. It was determined that no precipitation (of AgCl) occurred by the addition of $AgNO_3$ to the wash water. [bmim][BF_4] was purchased from Solvent Innovation (stated purity >98%). The Cl^- content, measured with a Cl^--specific electrode using the standard addition method, was 20 ppm and 100 ppm for [bmim][PF_6] and [bmim][BF_4], respectively. To reduce the water content and volatile compounds to negligible values, vacuum (0.1 Pa) and moderate temperature (60 °C) were applied to the [bmim][PF_6] and [bmim][BF_4] samples for several days always immediately prior to their use. The samples were analyzed by Karl Fisher titration and showed a mass % of water lower than 75 ppm ("Crison" Karl Fischer titration) and (70 ± 10) ppm (coulometric "Aquapal" Karl Fischer) for both [bmim][PF_6] and [bmim][BF_4].

Results and Discussion

[bmim][PF₆]. Speed of sound measurements have been carried out in a broad range of temperature ($283 < T/K < 323$) and pressure ($0.1 < p/MPa < 150$), sometimes inside the metastable, supercooled liquid region. Figure 1 and Table 1 report the speed of sound behavior as pressure and temperature change for [bmim][PF_6]. For the sake of economy, data are presented at nominal temperatures that typically differ from the actual ones by no more than 0.01 K.

Original data have been fitted to a Pade 3 × 3 equation of the form

$$(u/\mathrm{m\cdot s^{-1}}) = \frac{\sum_{i=0}^{2}\sum_{j=0}^{2} a_{ij}(T/\mathrm{K})^i(p/\mathrm{MPa})^j}{\sum_{k=0}^{2}\sum_{l=0}^{2} b_{kl}(T/\mathrm{K})^k(p/\mathrm{MPa})^l} \quad (1)$$

The values of the coefficients were calculated by means of a least-squares analysis of the experimental results (using the algorithm of Marquardt−Levenberg) and are given in Table 2. The standard deviation between the experimental and fitted values is found to be 0.07%. This fitting equation was screened for 40 isotherms within the experimental temperature range ($283 < T/K < 323$), thus in steps of 1 K, and for steps of 0.1 MPa within the

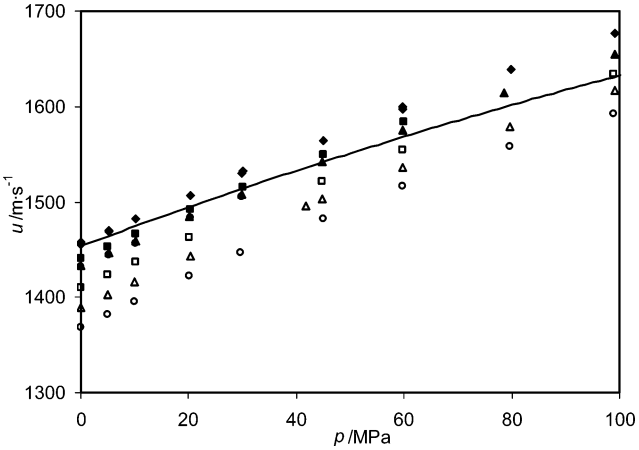

Figure 1. Isotherms of the experimental speed of sound of [bmim][PF_6]. The line represents the border between the stable and metastable, supercooled liquid. (See the text.) ◆, 283.16 K; ■, 291.15 K; ▲, 293.16 K; □, 303.16 K; △, 313.16 K; ○, 323.15 K.

Table 1. Experimental Speed of Sound, *u*, Data for [bmim][PF_6] as a Function of Temperature, *T*, and Pressure, *p*

p/MPa	*u*/m·s⁻¹	*p*/MPa	*u*/m·s⁻¹	*p*/MPa	*u*/m·s⁻¹
T = 283.16 K		*T* = 293.16 K		98.921	1634.38
0.100	1455.52	0.100	1432.85		
0.100	1457.60	5.157	1446.45	*T* = 313.16 K	
5.088	1468.58	10.195	1459.01	0.100	1389.49
5.131	1470.64	20.215	1484.18	5.010	1402.83
10.263	1481.79	29.959	1507.92	10.043	1416.43
20.249	1506.72	44.757	1542.20	20.319	1443.30
29.954	1529.87	59.732	1574.70	41.702	1495.14
29.995	1532.46	78.627	1613.77	44.866	1502.87
44.961	1564.25	99.149	1654.46	59.754	1536.27
59.682	1596.68			79.721	1578.64
59.829	1599.61	*T* = 294.16 K		99.097	1617.38
79.904	1638.64	0.100	1431.59	125.283	1662.16
99.077	1677.06	5.125	1444.54		
124.179	1724.36	10.105	1457.17	*T* = 323.25 K	
150.925	1772.61	20.357	1483.23	0.100	1367.98
		29.785	1506.04	5.061	1381.82
T = 291.15 K				9.942	1395.37
0.100	1440.19	*T* = 303.16 K		20.234	1422.72
5.069	1453.26	0.100	1410.27	29.721	1446.75
10.166	1466.63	5.078	1423.48	44.935	1482.19
20.400	1492.36	10.204	1437.13	59.711	1515.95
30.019	1515.72	20.225	1462.82	79.553	1557.89
44.920	1549.95	44.714	1521.26	98.901	1592.52
59.912	1583.22	59.773	1554.58		

Table 2. Coefficients of Equation 1 for *T*/K, *p*/MPa, and *u*/m·s⁻¹ within the Interval (283 < *T*/K < 323, 0.1 < *p*/MPa < 100)

a_{ij}	*j*		
i	0	1	2
0	-2.98041×10^4	6.35774×10^1	-1.53934×10^{-1}
1	−5.78316	8.03545×10^{-1}	9.68016×10^{-3}
2	4.03798×10^{-1}	-3.61889×10^{-3}	-3.23951×10^{-5}
b_{kl}	*L*		
k	0	1	2
0	1.00000	-1.66204×10^{-1}	2.51840×10^{-5}
1	-1.56369×10^{-1}	2.30593×10^{-3}	3.04219×10^{-6}
2	5.47760×10^{-4}	-6.07700×10^{-6}	-1.11069×10^{-8}

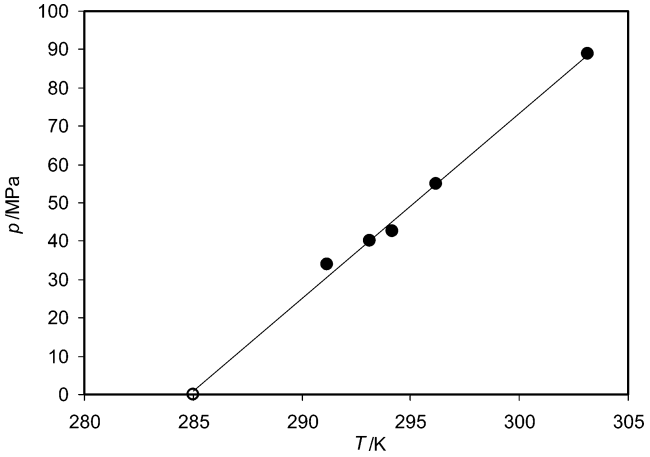

Figure 2. Melting line of [bmim][PF_6]. ●, Acoustic determinations. ○, Visual determination.

Table 3. $T-p$ Melting-Line Data of [bmim][PF_6]

T/K	p/MPa
285.00	0.1
291.15	34.0
293.15	40.2
294.16	42.5
296.15	55.0
303.15	88.9

experimental interval of pressure ($0.1 < p/\text{MPa} < 100$) for a total of 41 000 data points. No poles for this rational function were found. Also, neither the temperature nor the pressure derivatives of $u(p,T)$ as described by eq 1 present any anomalies. Therefore, eq 1 can be safely used for interpolations. It is already well known that ILs are relatively easy to metastabilize, meaning that, on cooling, they may remain liquid below their equilibrium melting line (supercooling). A liquid is said to be supercooled when it is found as such either at temperatures lower than those of the melting line or at pressures above it (for positively sloped melting lines). In the case of [bmim][PF_6], we have witnessed solidification several times in our isothermal runs intended to determine the speed of sound as a function of pressure. Because a crystalline phase cannot be superheated,[16] whenever solidification occurred we decided to lower the pressure slowly until the liquid state was again restored. Thus, we were able to detect several points of the melting line of [bmim][PF_6], since the difference between the speed of sound in this IL between the two states (solid versus liquid) is significant ($u_{sol} - u_{liq} \approx 1000$ ms^{-1}). Figure 2 and Table 3 present the solid/liquid phase transition line. Within the experimental uncertainty (±0.1 K, ±10 bar), the $p-T$ melting line shows linear behavior between coordinates (285.0 K, 0.1 MPa) and (303.15 K, 89.6 MPa), evolving with a slope of $dp/dT = 4.87$ MPa·K^{-1}. The first coordinate corresponds to our visual determination of melting at atmospheric pressure obtained in a sealed glass vessel by multiple cycles of slow temperature change. It agrees reasonably well with two values (283.15 K[17] and 283.51 K[18]) reported, but not with the one (276.43 K[19]) for water-free [bmim][PF_6]. It disagrees with that reported (277.15 K[17]) for water-equilibrated [bmim][PF_6]. The Clayperon equation can now be used to calculate the volume change on melting provided that one knows the corresponding enthalpy change. We note that literature values do not agree. Although Magee et al.[18] report a value of 19.6 kJ mol^{-1}, Domanska and Marciniak[19] determined a value of 9.21 kJ mol^{-1}. In our calculations, we have chosen the first value because their melting temperature agrees reasonably well with ours. Solidification in [bmim][PF_6] is accompanied by a contraction of about 7% ($\Delta V_S = -14.1$ cm^3·mol^{-1}). This value is highly dependent on the standardization of the enthalpy of fusion.

Table 4. Coefficients of Second-Order Polynomial Fits, $Y = A + B(T/\text{K}) + C(T/\text{K})^2$, to Atmospheric Isobars of $Y = \rho$ or $Y = C_p$

	ρ/kg·m^{-3}	C_p/J·K^{-1}·kg^{-1}
A	1620.7039	−1641.9284
B	−0.87955633	17.750623
C	8.4814007×10^{-5}	$-2.4889525 \times 10^{-2}$

The use of the speed of sound data to derive other thermodynamic properties requires a knowledge of one isobar of both density and heat capacity. There are already two sets of data available from different groups.[4,18,20] The choice of the isobars for the thermodynamic properties calculations was based on the comparison of both density and isobaric heat capacity data. The values presented by Magee et al.[18] seem more precise and are greater than those of Gu et al.[20] and Fredlake et al.[4] for both quantities (which may possibly be an indication of higher sample purity because it is quite uncommon to find typical impurities that are responsible for the increase in these properties). However, despite the fact that, in turn, these densities[18] are slightly lower than those presented by us[3,21] (for about 0.1%) and by Tokuda et al.[5] (for about 0.35%), that is the best set of combined data of densities and heat capacities along one isobar.

The atmospheric isobars of both density and heat capacity[18] were fitted with a second-order polynomial equation up to 330 K. The coefficients of the fittings are shown in Table 4. The method used to derive other thermodynamic properties is based on well-established thermodynamic relations. The speed of sound, u, is directly related to the pressure derivative of the density, ρ, through eq 2, in which the subscript S denotes the condition of constant entropy.

$$\left(\frac{\partial\rho}{\partial p}\right)_S = \frac{1}{u^2} \tag{2}$$

This derivative is related to the isothermal pressure derivative and the isobaric temperature derivative of the density through eq 3, where C_p is the specific heat capacity at constant pressure.

$$\left(\frac{\partial\rho}{\partial p}\right)_S = \left(\frac{\partial\rho}{\partial p}\right)_T - \frac{T}{\rho^2 C_p}\left(\frac{\partial\rho}{\partial T}\right)_p^2 \tag{3}$$

Rearranging the last equation and combining it with eq 2 creates eq 4, which also incorporates the definition of the thermal expansion coefficient, α_p:

$$\left(\frac{\partial\rho}{\partial p}\right)_T = \frac{1}{u^2} + \frac{T}{C_p}\alpha_p^2 \tag{4}$$

$$\alpha_p = -\frac{1}{\rho}\left(\frac{\partial\rho}{\partial T}\right)_p \tag{5}$$

It can also be shown that the isothermal pressure partial derivative of the isobaric heat capacity can be calculated with eq 6:

$$\left(\frac{\partial C_p}{\partial p}\right)_T = -\frac{T}{\rho}\left[\alpha_p^2 + \left(\frac{\partial\alpha_p}{\partial T}\right)_p\right] \tag{6}$$

Thus, given an isobar of the density and of C_p, it is possible to integrate eqs 4 and 6 over pressure,[22] thus obtaining the (p, ρ, T) and (p, C_p, T) surfaces within the

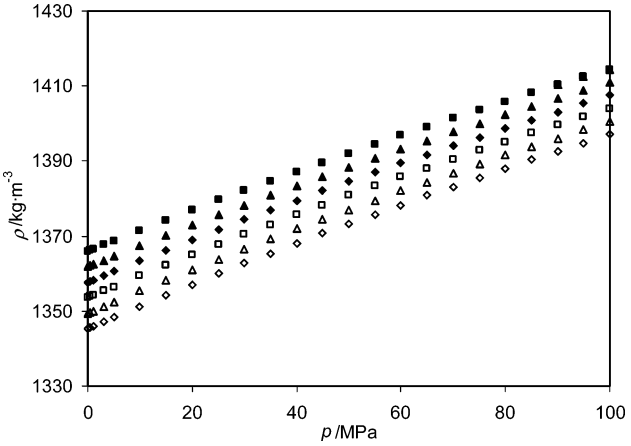

Figure 3. Isotherms for the density of [bmim][PF_6]. ■, 298.15 K; ▲, 303.15 K; ◆, 308.15 K; □, 313.15 K; △, 318.15 K; ◇, 323.15 K.

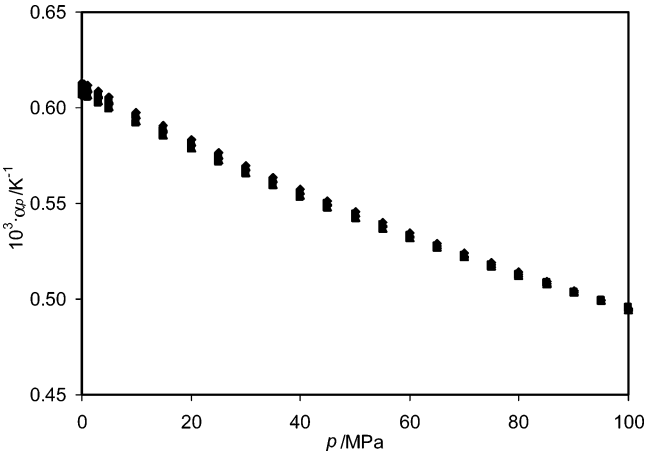

Figure 4. Isotherms for the isobaric expansivity of [bmim][PF_6]. ■, 298.15 K; ▲, 303.15 K; ◆, 308.15 K; □, 313.15 K; △, 318.15 K; ◇, 323.15 K.

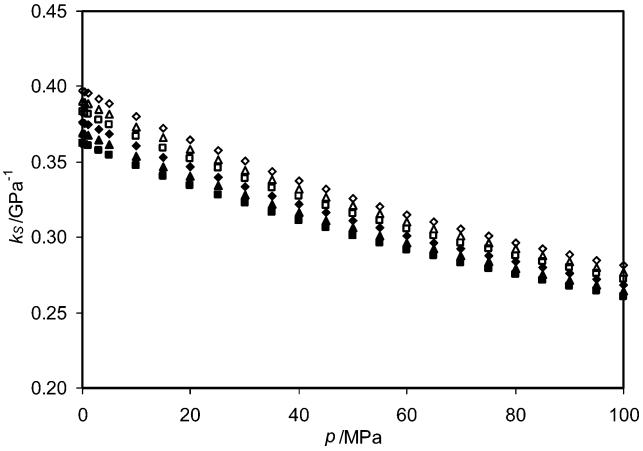

Figure 5. Isotherms for the isentropic compressibility of [bmim][PF_6]. ■, 298.15 K; ▲, 303.15 K; ◆, 308.15 K; □, 313.15 K; △, 318.15 K; ◇, 323.15 K.

range of pressure and temperature of the experimental speed of sound data. The numerical integration procedure also allows one to calculate other properties, such as the isentropic compressibility, κ_S, isothermal compressibility, κ_T, isobaric thermal expansivity, α_p, isochoric heat capacity C_v, and thermal pressure coefficient, γ_v. The estimated overall uncertainties (including sample impurities) are as follows: isentropic compressibility, κ_S (1%); isothermal compressibility, κ_T (2%); isobaric thermal expansivity, α_p

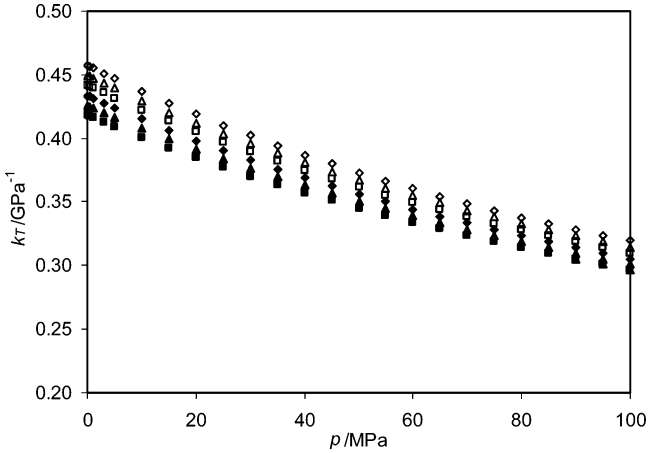

Figure 6. Isotherms for the isothermal compressibility of [bmim][PF_6]. ■, 298.15 K; ▲, 303.15 K; ◆, 308.15 K; □, 313.15 K; △, 318.15 K; ◇, 323.15 K.

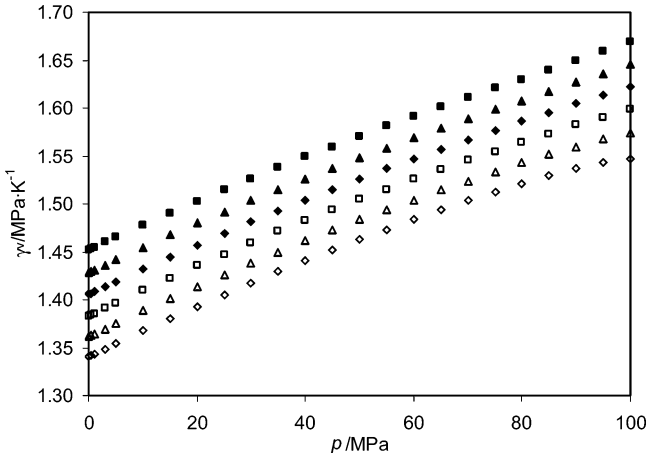

Figure 7. Isotherms for the thermal pressure coefficient of [bmim][PF_6]. ■, 298.15 K; ▲, 303.15 K; ◆, 308.15 K; □, 313.15 K; △, 318.15 K; ◇, 323.15 K.

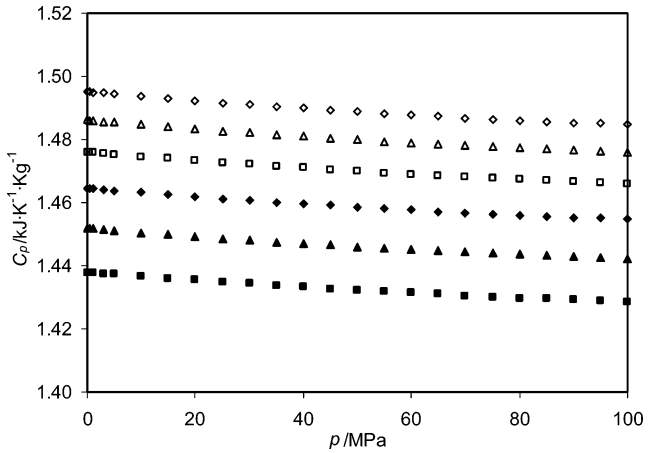

Figure 8. Isotherms for the isobaric heat capacity of [bmim][PF_6]. ■, 298.15 K; ▲, 303.15 K; ◆, 308.15 K; □, 313.15 K; △, 318.15 K; ◇, 323.15 K.

(4%); isobaric heat capacity, C_p (5%); isochoric heat capacity, C_v (8%); and thermal pressure coefficient, γ_v (6%). It should be noted that in the case of heat capacities the major contribution to the uncertainty lies in that of the original calorimetric data. The integration was carried out from atmospheric pressure up to 100 MPa. The results obtained for several thermodynamic properties are presented in Figures 3 to 9 and Tables 5 to 11.

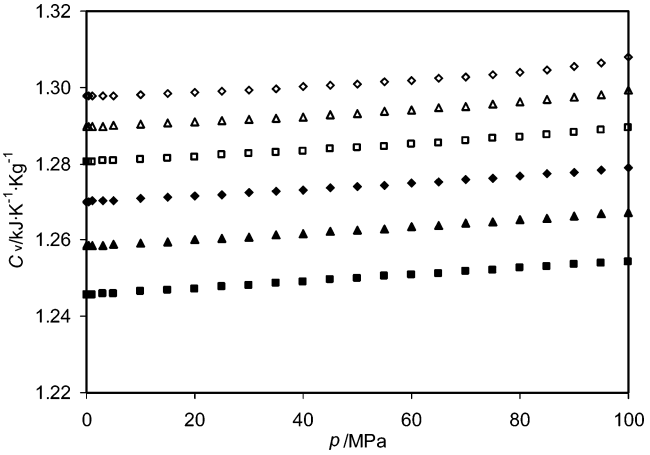

Figure 9. Isotherms for the isochoric heat capacity of [bmim][PF_6]. ■, 298.15 K; ▲, 303.15 K; ◆, 308.15 K; □, 313.15 K; △, 318.15 K; ◇, 323.15 K.

The isothermal compressibility results can be compared with those of Gu et al.[20] showing deviations that go from −1% at atmospheric pressure to +12% at 100 MPa and 298.2 K and from −9% to +13% at 323.2 K.

As for the heat capacities, results for both the isobaric and isochoric heat capacities reveal, in practice, pressure independence.

Although expansivities decrease markedly with pressure, according to Figure 4 and Table 8 they present a tendency to increase very mildly with increasing temperature at constant pressure. This trend agrees with that reported by Tokuda et al.[5] at atmospheric pressure. Nonetheless, within the typical experimental uncertainty of α_p calculations (4%) the expansivities of [bmim][PF_6] can, in practice, be considered almost temperature-independent. This behavior contradicts that which has been reported in other works[18,20] in which α_p of [bmim][PF_6] decreases as temperature rises. This contradiction underlies numerical difficulties in the data evaluation associated with very subtle effects and was previously noticed in different communications[3,6,23]. The point is that a detailed evaluation of the raw data reveals that deviations from linearity in density−temperature (or volume−temperature) plots are so mild that the determination of the temperature coefficient of α_p

Table 5. Calculated Values of Density, ρ, for [bmim][PF_6]

	T/K							*T*/K					
p/MPa	298.15	303.15	308.15	313.15	318.15	323.15	*p*/MPa	298.15	303.15	308.15	313.15	318.15	323.15
	ρ/kg·m^{-3}							ρ/kg·m^{-3}					
0.1	1366.0_0	1361.8_6	1357.7_2	1353.5_9	1349.4_6	1345.3_3	45	1389.6_4	1385.8_4	1382.0_4	1378.2_5	1374.4_6	1370.6_8
0.5	1366.2_3	1362.0_9	1357.9_6	1353.8_3	1349.7_0	1345.5_8	50	1392.0_6	1388.2_9	1384.5_3	1380.7_7	1377.0_1	1373.2_6
1	1366.5_2	1362.3_8	1358.2_5	1354.1_2	1350.0_0	1345.8_8	55	1394.4_5	1390.7_1	1386.9_7	1383.2_5	1379.5_2	1375.8_1
3	1367.6_5	1363.5_3	1359.4_2	1355.3_1	1351.2_1	1347.1_1	60	1396.8_0	1393.0_9	1389.3_8	1385.6_9	1381.9_9	1378.3_1
5	1368.7_7	1364.6_7	1360.5_8	1356.4_9	1352.4_0	1348.3_2	65	1399.1_1	1395.4_3	1391.7_6	1388.0_9	1384.4_3	1380.7_7
10	1371.5_5	1367.4_9	1363.4_3	1359.3_9	1355.3_4	1351.3_0	70	1401.4_0	1397.7_4	1394.1_0	1390.4_6	1386.8_3	1383.2_0
15	1374.2_7	1370.2_5	1366.2_4	1362.2_3	1358.2_2	1354.2_2	75	1403.6_5	1400.0_3	1396.4_1	1392.8_0	1389.1_9	1385.5_9
20	1376.9_4	1372.9_6	1368.9_9	1365.0_2	1361.0_5	1357.0_9	80	1405.8_7	1402.2_8	1398.6_9	1395.1_0	1391.5_2	1387.9_5
25	1379.5_7	1375.6_3	1371.6_9	1367.7_6	1363.8_3	1359.9_1	85	1408.0_7	1404.5_0	1400.9_3	1397.3_8	1393.8_3	1390.2_8
30	1382.1_5	1378.2_4	1374.3_4	1370.4_5	1366.5_6	1362.6_7	90	1410.2_3	1406.6_9	1403.1_5	1399.6_2	1396.1_0	1392.5_8
35	1384.6_9	1380.8_2	1376.9_5	1373.0_9	1369.2_4	1365.3_9	95	1412.3_7	1408.8_5	1405.3_4	1401.8_3	1398.3_4	1394.8_5
40	1387.1_8	1383.3_5	1379.5_2	1375.6_9	1371.8_7	1368.0_6	100	1414.4_9	1410.9_9	1407.5_0	1404.0_2	1400.5_5	1397.1_0

Table 6. Calculated Values of κ_T for [bmim][PF_6]

	T/K							*T*/K					
p/MPa	298.15	303.15	308.15	313.15	318.15	323.15	*p*/MPa	298.15	303.15	308.15	313.15	318.15	323.15
	κ_T/GPa^{-1}							κ_T/GPa^{-1}					
0.1	0.417_9	0.425_6	0.433_5	0.441_4	0.449_3	0.457_3	45	0.351_0	0.356_7	0.362_4	0.368_1	0.374_0	0.379_8
0.5	0.417_1	0.424_9	0.432_7	0.440_6	0.448_5	0.456_4	50	0.345_1	0.350_6	0.356_1	0.361_7	0.367_3	0.373_0
1	0.416_2	0.423_9	0.431_7	0.439_6	0.447_4	0.455_4	55	0.339_5	0.344_8	0.350_1	0.355_5	0.361_0	0.366_5
3	0.412_6	0.420_2	0.427_9	0.435_6	0.443_4	0.451_2	60	0.334_0	0.339_1	0.344_3	0.349_6	0.354_9	0.360_3
5	0.409_1	0.416_6	0.424_1	0.431_7	0.439_4	0.447_1	65	0.328_8	0.333_8	0.338_8	0.343_9	0.349_1	0.354_3
10	0.400_6	0.407_8	0.415_1	0.422_4	0.429_7	0.437_2	70	0.323_7	0.328_6	0.333_5	0.338_4	0.343_5	0.348_6
15	0.392_5	0.399_4	0.406_4	0.413_5	0.420_6	0.427_7	75	0.318_9	0.323_6	0.328_4	0.333_2	0.338_1	0.343_1
20	0.384_8	0.391_5	0.398_2	0.405_0	0.411_9	0.418_8	80	0.314_2	0.318_8	0.323_4	0.328_1	0.332_9	0.337_8
25	0.377_4	0.383_9	0.390_4	0.397_0	0.403_6	0.410_2	85	0.309_7	0.314_1	0.318_6	0.323_2	0.327_9	0.332_8
30	0.370_3	0.376_6	0.382_9	0.389_3	0.395_7	0.402_1	90	0.305_4	0.309_7	0.314_0	0.318_5	0.323_2	0.328_0
35	0.363_6	0.369_7	0.375_8	0.381_9	0.388_1	0.394_3	95	0.301_1	0.305_3	0.309_5	0.313_9	0.318_6	0.323_5
40	0.357_2	0.363_0	0.368_9	0.374_9	0.380_9	0.386_9	100	0.297_1	0.301_0	0.305_1	0.309_5	0.314_2	0.319_5

Table 7. Calculated Values of κ_S for [bmim][PF_6]

	T/K							*T*/K					
p/MPa	298.15	303.15	308.15	313.15	318.15	323.15	*p*/MPa	298.15	303.15	308.15	313.15	318.15	323.15
	κ_S/GPa^{-1}							κ_S/GPa^{-1}					
0.1	0.362_0	0.368_9	0.375_9	0.382_9	0.389_9	0.396_9	45	0.306_1	0.311_2	0.316_3	0.321_4	0.326_5	0.331_7
0.5	0.361_3	0.368_3	0.375_3	0.382_3	0.389_2	0.396_2	50	0.301_2	0.306_1	0.311_1	0.316_0	0.321_0	0.326_0
1	0.360_6	0.367_5	0.374_5	0.381_4	0.388_4	0.395_3	55	0.296_4	0.301_2	0.306_0	0.310_8	0.315_7	0.320_5
3	0.357_6	0.364_4	0.371_3	0.378_1	0.384_9	0.391_8	60	0.291_9	0.296_5	0.301_2	0.305_9	0.310_6	0.315_3
5	0.354_6	0.361_4	0.368_1	0.374_8	0.381_6	0.388_3	65	0.287_5	0.292_0	0.296_5	0.301_1	0.305_7	0.310_3
10	0.347_5	0.354_0	0.360_5	0.367_0	0.373_5	0.379_9	70	0.283_3	0.287_7	0.292_1	0.296_5	0.301_0	0.305_5
15	0.340_8	0.347_0	0.353_3	0.359_5	0.365_8	0.372_0	75	0.279_2	0.283_5	0.287_8	0.292_1	0.296_4	0.300_9
20	0.334_3	0.340_3	0.346_4	0.352_4	0.358_4	0.364_5	80	0.275_3	0.279_4	0.283_6	0.287_8	0.292_1	0.296_5
25	0.328_2	0.334_0	0.339_8	0.345_6	0.351_5	0.357_3	85	0.271_5	0.275_5	0.279_6	0.283_7	0.287_9	0.292_2
30	0.322_3	0.327_9	0.333_5	0.339_2	0.344_8	0.350_4	90	0.267_9	0.271_8	0.275_7	0.279_8	0.283_9	0.288_3
35	0.316_7	0.322_1	0.327_5	0.333_0	0.338_4	0.343_9	95	0.264_3	0.268_1	0.272_0	0.275_9	0.280_1	0.284_6
40	0.311_3	0.316_5	0.321_8	0.327_1	0.332_4	0.337_6	100	0.260_8	0.264_5	0.268_2	0.272_2	0.276_6	0.281_5

Table 8. Calculated Values of α_p for [bmim][PF_6]

	T/K							*T*/K					
p/MPa	298.15	303.15	308.15	313.15	318.15	323.15	*p*/MPa	298.15	303.15	308.15	313.15	318.15	323.15
				$10^3\alpha_p/K^{-1}$							$10^3\alpha_p/K^{-1}$		
0.1	0.606_9	0.608_1	0.609_3	0.610_6	0.611_8	0.613_0	45	0.547_5	0.548_3	0.549_1	0.549_9	0.550_7	0.551_5
0.5	0.606_3	0.607_5	0.608_7	0.609_9	0.611_2	0.612_4	50	0.542_0	0.542_7	0.543_5	0.544_2	0.544_9	0.545_7
1	0.605_5	0.606_7	0.607_9	0.609_1	0.610_4	0.611_6	55	0.536_6	0.537_3	0.538_0	0.538_7	0.539_3	0.540_0
3	0.602_4	0.603_6	0.604_8	0.606_0	0.607_2	0.608_4	60	0.531_5	0.532_1	0.532_7	0.533_3	0.533_9	0.534_5
5	0.599_4	0.600_6	0.601_8	0.602_9	0.604_1	0.605_3	65	0.526_4	0.527_0	0.527_5	0.528_1	0.528_6	0.529_2
10	0.592_1	0.593_2	0.594_3	0.595_5	0.596_6	0.597_8	70	0.521_6	0.522_0	0.522_5	0.523_0	0.523_5	0.524_0
15	0.585_0	0.586_1	0.587_2	0.588_3	0.589_4	0.590_4	75	0.516_8	0.517_2	0.517_7	0.518_1	0.518_5	0.518_9
20	0.578_2	0.579_2	0.580_3	0.581_3	0.582_3	0.583_4	80	0.512_3	0.512_6	0.512_9	0.513_3	0.513_6	0.513_9
25	0.571_6	0.572_6	0.573_6	0.574_6	0.575_6	0.576_6	85	0.507_8	0.508_1	0.508_3	0.508_6	0.508_8	0.509_0
30	0.565_3	0.566_2	0.567_2	0.568_1	0.569_1	0.570_0	90	0.503_6	0.503_7	0.503_8	0.503_9	0.504_1	0.504_2
35	0.559_2	0.560_1	0.561_0	0.561_8	0.562_7	0.563_6	95	0.499_5	0.499_5	0.499_4	0.499_4	0.499_3	0.499_3
40	0.553_3	0.554_1	0.554_9	0.555_8	0.556_6	0.557_4	100	0.495_7	0.495_4	0.495_1	0.494_8	0.494_5	0.494_3

Table 9. Calculated Values of γ_v for [bmim][PF_6]

	T/K							*T*/K					
p/MPa	298.15	303.15	308.15	313.15	318.15	323.15	*p*/MPa	298.15	303.15	308.15	313.15	318.15	323.15
				γ_v/MPa·K^{-1}							γ_v/MPa·K^{-1}		
0.1	1.45_2	1.42_9	1.40_6	1.38_3	1.36_2	1.34_1	45	1.56_0	1.53_7	1.51_5	1.49_4	1.47_3	1.45_2
0.5	1.45_3	1.43_0	1.40_7	1.38_4	1.36_3	1.34_2	50	1.57_0	1.54_8	1.52_6	1.50_5	1.48_3	1.46_3
1	1.45_5	1.43_1	1.40_8	1.38_6	1.36_4	1.34_3	55	1.58_1	1.55_9	1.53_7	1.51_5	1.49_4	1.47_3
3	1.46_0	1.43_6	1.41_3	1.39_1	1.37_0	1.34_9	60	1.59_1	1.56_9	1.54_7	1.52_5	1.50_4	1.48_4
5	1.46_5	1.44_2	1.41_9	1.39_7	1.37_5	1.35_4	65	1.60_1	1.57_9	1.55_7	1.53_5	1.51_4	1.49_3
10	1.47_8	1.45_5	1.43_2	1.41_0	1.38_8	1.36_7	70	1.61_1	1.58_9	1.56_7	1.54_5	1.52_4	1.50_3
15	1.49_1	1.46_7	1.44_5	1.42_3	1.40_1	1.38_0	75	1.62_1	1.59_8	1.57_7	1.55_5	1.53_4	1.51_2
20	1.50_3	1.48_0	1.45_7	1.43_5	1.41_4	1.39_3	80	1.63_0	1.60_8	1.58_6	1.56_4	1.54_3	1.52_1
25	1.51_5	1.49_2	1.46_9	1.44_8	1.42_6	1.40_5	85	1.64_0	1.61_7	1.59_5	1.57_3	1.55_1	1.53_0
30	1.52_6	1.50_4	1.48_1	1.45_9	1.43_8	1.41_8	90	1.64_9	1.62_7	1.60_4	1.58_2	1.56_0	1.53_7
35	1.53_8	1.51_5	1.49_3	1.47_1	1.45_0	1.42_9	95	1.65_9	1.63_6	1.61_3	1.59_1	1.56_8	1.54_4
40	1.54_9	1.52_6	1.50_4	1.48_3	1.46_1	1.44_1	100	1.66_9	1.64_6	1.62_3	1.59_9	1.57_4	1.54_7

Table 10. Calculated Values of C_p for [bmim][PF_6]

	T/K							*T*/K					
p/MPa	298.15	303.15	308.15	313.15	318.15	323.15	*p*/MPa	298.15	303.15	308.15	313.15	318.15	323.15
				C_p/kJ·K^{-1}·kg^{-1}							C_p/kJ·K^{-1}·kg^{-1}		
0.1	1.43_8	1.45_2	1.46_5	1.47_6	1.48_6	1.49_5	45	1.43_3	1.44_7	1.45_9	1.47_0	1.48_0	1.48_9
0.5	1.43_8	1.45_2	1.46_4	1.47_6	1.48_6	1.49_5	50	1.43_2	1.44_6	1.45_9	1.47_0	1.48_0	1.48_9
1	1.43_8	1.45_2	1.46_4	1.47_6	1.48_6	1.49_5	55	1.43_2	1.44_6	1.45_8	1.46_9	1.47_9	1.48_8
3	1.43_8	1.45_1	1.46_4	1.47_6	1.48_6	1.49_5	60	1.43_1	1.44_5	1.45_8	1.46_9	1.47_9	1.48_8
5	1.43_7	1.45_1	1.46_4	1.47_5	1.48_5	1.49_4	65	1.43_1	1.44_5	1.45_7	1.46_8	1.47_9	1.48_7
10	1.43_7	1.45_1	1.46_3	1.47_5	1.48_5	1.49_4	70	1.43_1	1.44_4	1.45_7	1.46_8	1.47_8	1.48_7
15	1.43_6	1.45_0	1.46_3	1.47_4	1.48_4	1.49_3	75	1.43_0	1.44_4	1.45_6	1.46_8	1.47_8	1.48_6
20	1.43_5	1.44_9	1.46_2	1.47_3	1.48_3	1.49_2	80	1.43_0	1.44_4	1.45_6	1.46_7	1.47_7	1.48_6
25	1.43_5	1.44_9	1.46_1	1.47_3	1.48_3	1.49_2	85	1.42_9	1.44_3	1.45_6	1.46_7	1.47_7	1.48_6
30	1.43_4	1.44_8	1.46_1	1.47_2	1.48_2	1.49_1	90	1.42_9	1.44_3	1.45_5	1.46_7	1.47_7	1.48_5
35	1.43_4	1.44_8	1.46_0	1.47_1	1.48_2	1.49_0	95	1.42_9	1.44_3	1.45_5	1.46_6	1.47_6	1.48_5
40	1.43_3	1.44_7	1.46_0	1.47_1	1.48_1	1.49_0	100	1.42_9	1.44_2	1.45_5	1.46_6	1.47_6	1.48_5

Table 11. Calculated Values of C_v for [bmim][PF_6]

	T/K							*T*/K					
p/MPa	298.15	303.15	308.15	313.15	318.15	323.15	*p*/MPa	298.15	303.15	308.15	313.15	318.15	323.15
				C_v/kJ·K^{-1}·kg^{-1}							C_v/kJ·K^{-1}·kg^{-1}		
0.1	1.24_6	1.25_8	1.27_0	1.28_1	1.29_0	1.29_8	45	1.24_9	1.26_2	1.27_4	1.28_4	1.29_3	1.30_1
0.5	1.24_6	1.25_8	1.27_0	1.28_1	1.29_0	1.29_8	50	1.25_0	1.26_3	1.27_4	1.28_4	1.29_3	1.30_1
1	1.24_6	1.25_9	1.27_0	1.28_1	1.29_0	1.29_8	55	1.25_0	1.26_3	1.27_4	1.28_5	1.29_4	1.30_1
3	1.24_6	1.25_9	1.27_0	1.28_1	1.29_0	1.29_8	60	1.25_1	1.26_3	1.27_5	1.28_5	1.29_4	1.30_2
5	1.24_6	1.25_9	1.27_0	1.28_1	1.29_0	1.29_8	65	1.25_1	1.26_4	1.27_5	1.28_6	1.29_5	1.30_2
10	1.24_6	1.25_9	1.27_1	1.28_1	1.29_0	1.29_8	70	1.25_2	1.26_4	1.27_6	1.28_6	1.29_5	1.30_3
15	1.24_7	1.26_0	1.27_1	1.28_2	1.29_1	1.29_8	75	1.25_2	1.26_5	1.27_6	1.28_7	1.29_6	1.30_3
20	1.24_7	1.26_0	1.27_2	1.28_2	1.29_1	1.29_9	80	1.25_3	1.26_5	1.27_7	1.28_7	1.29_6	1.30_4
25	1.24_8	1.26_0	1.27_2	1.28_2	1.29_1	1.29_9	85	1.25_3	1.26_6	1.27_7	1.28_8	1.29_7	1.30_5
30	1.24_8	1.26_1	1.27_2	1.28_3	1.29_2	1.29_9	90	1.25_4	1.26_6	1.27_8	1.28_8	1.29_7	1.30_5
35	1.24_9	1.26_1	1.27_3	1.28_3	1.29_2	1.30_0	95	1.25_4	1.26_7	1.27_8	1.28_9	1.29_8	1.30_6
40	1.24_9	1.26_2	1.27_3	1.28_3	1.29_2	1.30_0	100	1.25_4	1.26_7	1.27_9	1.29_0	1.29_9	1.30_8

is extremely dependent on the choice of the type of function to screen the data. For those situations where the statistical scatter of the raw data is large compared with an unambiguous determination of the curvature, we suggest the use of $\ln \rho = f(T)$. If this function proves to be linear, then $\ln V = f(T)$ is as well, and α_p is constant (temperature-independent). Moreover, the choice of a logarithmic function avoids the existence of a mathematical violation that arises if one considers that both $\rho-T$ and $V-T$ plots are linear.

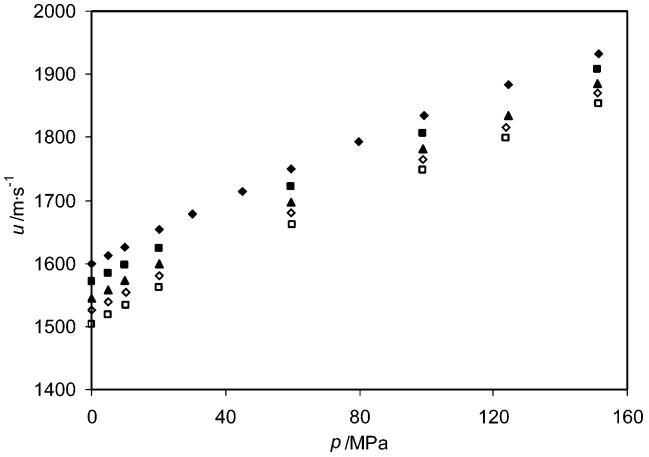

Figure 10. Isotherms for the experimental speed of sound in [bmim][BF_4]. ◆, 283.15 K; ■, 293.15 K; ▲, 303.15 K; ◇, 313.15 K; □, 323.15 K.

Table 12. Experimental Speed of Sound, *u*, Data for [bmim][BF_4] as a Function of Temperature, *T*, and Pressure, *p*

p/MPa	*u*/m·s^{-1}	*p*/MPa	*u*/m·s^{-1}	*p*/MPa	*u*/m·s^{-1}
T = 283.15 K		20.080	1624.43	10.185	1554.04
0.100	1599.51	59.673	1721.05	20.070	1580.96
4.956	1612.54	98.994	1806.08	59.719	1679.35
9.954	1626.20	151.068	1907.30	99.014	1765.79
20.130	1653.13			123.975	1816.59
30.003	1678.26	*T* = 303.15 K		151.204	1869.96
44.948	1714.66	0.100	1544.88		
59.705	1749.05	5.080	1558.60	*T* = 323.15 K	
79.788	1793.04	10.091	1572.45	0.100	1503.36
99.235	1833.62	20.063	1599.53	4.999	1517.83
124.380	1882.86	59.767	1697.00	10.202	1533.40
151.416	1932.20	99.007	1782.61	20.046	1561.37
		124.609	1834.02	59.977	1662.08
T = 293.15 K				99.014	1748.81
0.100	1570.23	*T* = 313.15 K		123.945	1798.92
5.094	1583.99	0.100	1525.22	151.374	1853.24
10.075	1597.70	5.091	1539.35		

Table 13. Coefficients of Equation 1 for *T*/K, *p*/MPa, and *u*/m·s^{-1} within the Interval (283 < *T*/K < 323, 0.1 < *p*/MPa < 100)

a_{ij}	*j*		
i	0	1	2
0	1.11539×10^{3}	1.16241×10^{1}	-1.85200×10^{-2}
1	-1.03226×10^{1}	-8.64584×10^{-2}	1.23988×10^{-4}
2	2.10054×10^{-2}	1.55385×10^{-4}	-2.03876×10^{-7}
b_{kl}	*L*		
k	0	1	2
0	1.00000	5.81502×10^{-3}	-1.49739×10^{-5}
1	-8.43584×10^{-3}	-4.13259×10^{-5}	9.95819×10^{-8}
2	1.63578×10^{-5}	7.19818×10^{-8}	-1.63623×10^{-10}

[bmim][BF_4]. Speed of sound measurements have been carried out at broad ranges of temperature (283 < *T*/K < 323) and pressure (0.1 < *p*/MPa < 160). Figure 10 and Table 12 show the speed of sound behavior with pressure and temperature for [bmim][BF_4]. Equation 1 was used to fit the experimental data, and all of the tests proved the nonexistence of poles in the (*p*, *u*, *T*) surface considered. The values of the fitting coefficients are provided in Table 13. The standard deviation between the experimental and fitted values is found to be 0.04%.

Density measurements have been carried out at broad ranges of temperature (298 < *T*/K < 333) and pressure (0.1 < *p*/MPa < 60). The experimental data are presented both in Figure 11 and Table 14.

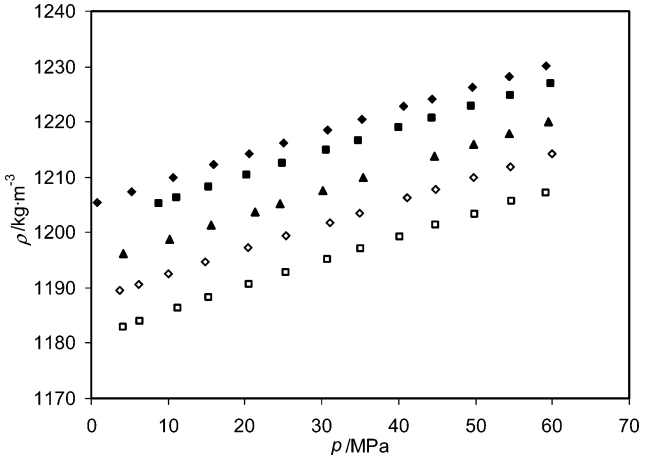

Figure 11. Isotherms for the experimental density of [bmim][BF_4]. ◆, 298.34 K; ■, 303.23 K; ▲, 313.01 K; ◇, 322.85 K; □, 332.73 K.

Table 14. Experimental Density, ρ, Data for [bmim][BF_4] as a Function of Temperature, *T*, and Pressure, *p*

p/MPa	ρ/kg·m^{-3}	*p*/MPa	ρ/kg·m^{-3}	*p*/MPa	ρ/kg·m^{-3}
T = 298.34 K		44.31	1220.61	25.40	1199.38
0.1	1205.03	49.50	1222.73	31.09	1201.87
0.70	1205.32	54.49	1224.75	34.85	1203.51
5.28	1207.44	59.82	1226.85	41.13	1206.23
10.60	1209.87			44.88	1207.85
15.92	1212.24	*T* = 313.01 K		49.83	1209.95
20.54	1214.26	0.1	1194.59	54.52	1211.91
25.00	1216.18	4.13	1196.19	59.92	1214.20
30.71	1218.62	10.18	1198.82		
35.19	1220.47	15.65	1201.26	*T* = 332.73 K	
40.66	1222.73	21.30	1203.75	0.1	1181.05
44.37	1224.21	24.58	1205.19	4.13	1182.92
49.66	1226.32	30.11	1207.62	6.35	1183.98
54.34	1228.16	35.39	1209.88	11.21	1186.30
59.23	1230.05	44.70	1213.84	15.22	1188.15
		49.72	1215.92	20.54	1190.55
T = 303.23 K		54.43	1217.91	25.28	1192.70
0.1	1201.29	59.45	1219.95	30.76	1195.16
8.78	1205.30			35.08	1197.05
11.17	1206.40	*T* = 322.85 K		40.11	1199.23
15.23	1208.22	0.1	1187.85	44.86	1201.24
20.27	1210.43	3.73	1189.50	49.84	1203.35
24.89	1212.44	6.22	1190.68	54.76	1205.70
30.67	1214.92	10.02	1192.47	59.13	1207.20
34.77	1216.66	14.87	1194.68		
40.02	1218.85	20.45	1197.20		

Table 15. Coefficients of Second-Order Polynomial Fits, $Y = A + B(T/\mathrm{K}) + C(T/\mathrm{K})^2$, to Atmospheric Isobars of $Y = \rho$ or $Y = C_p$

	ρ/kg·m^{-3}	C_p/J·K^{-1}·kg^{-1}
A	1476.2773	2056.7965
B	−1.1035102	−5.2008507
C	6.5020339×10^{-4}	1.2456247×10^{-2}

The derived thermodynamic properties were calculated by the integration method using isobaric density data of this current work and heat capacities taken from literature data[23] at 0.1 MPa. The atmospheric isobars of both density and heat capacity were fitted with a second-order polynomial equation. The coefficients of the fittings are reported in Table 15. The integration was carried out from atmospheric pressure up to 150 MPa. The results obtained for several thermodynamic properties are presented in Figures 12 to 17 and Tables 16 to 21.

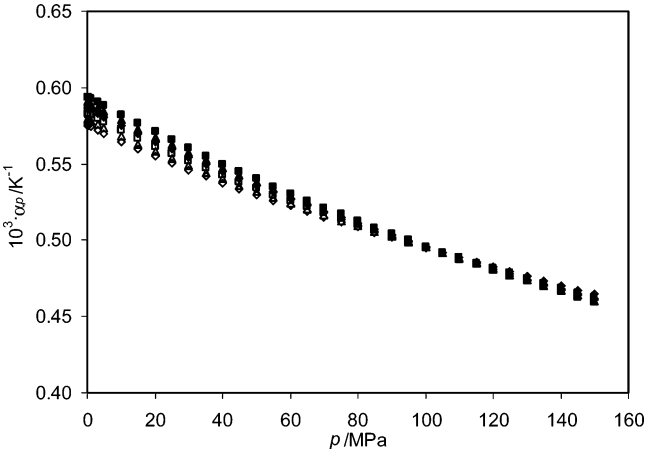

Figure 12. Isotherms for the isobaric expansivity of [bmim][BF_4]. ■, 298.15 K; ▲, 303.15 K; ◆, 308.15 K; □, 313.15 K; △, 318.15 K; ◇, 323.15 K.

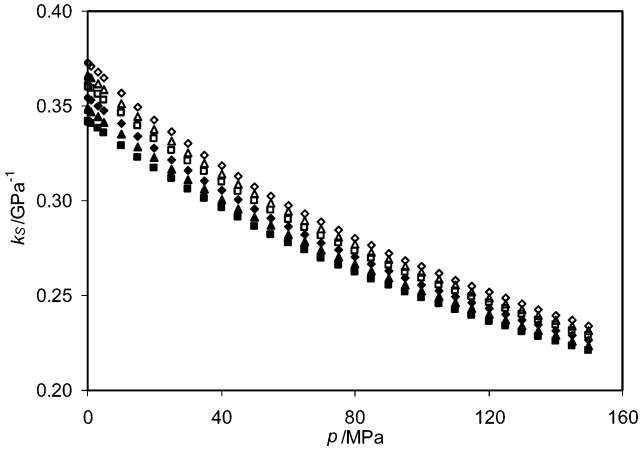

Figure 13. Isotherms for the isentropic compressibility of [bmim][BF_4]. ■, 298.15 K; ▲, 303.15 K; ◆, 308.15 K; □, 313.15 K; △, 318.15 K; ◇, 323.15 K.

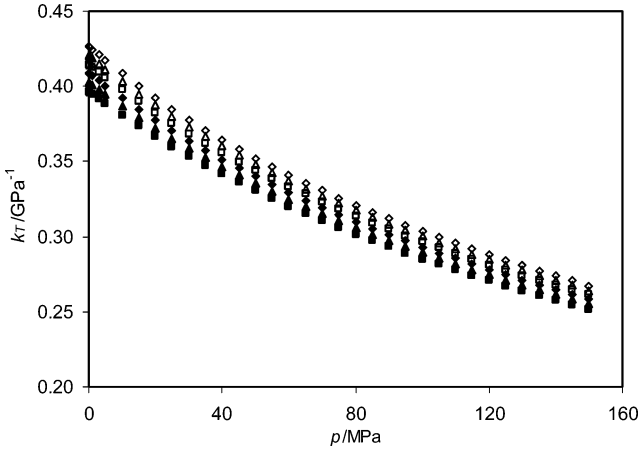

Figure 14. Isotherms for the isothermal compressibility of [bmim][BF_4]. ■, 298.15 K; ▲, 303.15 K; ◆, 308.15 K; □, 313.15 K; △, 318.15 K; ◇, 323.15 K.

The comparison between the density data taken from the integration procedure and the experimental ones shows good agreement with a maximum deviation smaller than 0.1%, even at pressures as high as 60 MPa. This deviation is small and can be ascribed to the uncertainty of the speed of sound measurements because this quantity is responsible for about 85% of the calculated dρ/dp in the integration process.

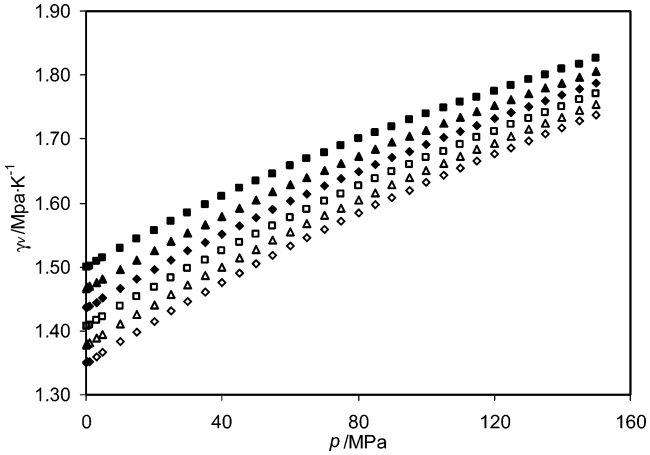

Figure 15. Isotherms for the thermal pressure coefficient of [bmim][BF_4]. ■, 298.15 K; ▲, 303.15 K; ◆, 308.15 K; □, 313.15 K; △, 318.15 K; ◇, 323.15 K.

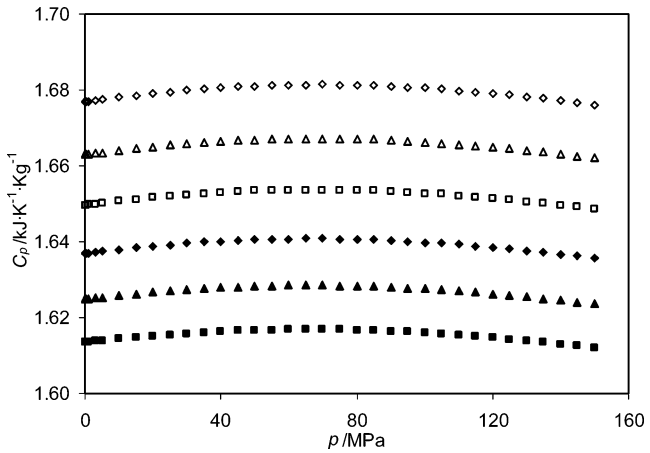

Figure 16. Isotherms for the isobaric heat capacity of [bmim][BF_4]. ■, 298.15 K; ▲, 303.15 K; ◆, 308.15 K; □, 313.15 K; △, 318.15 K; ◇, 323.15 K.

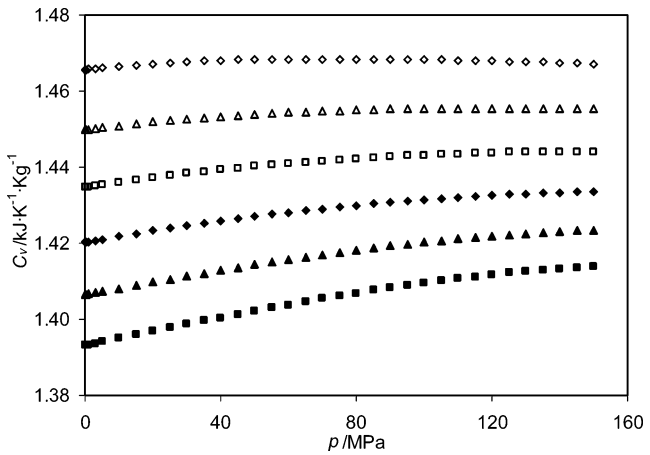

Figure 17. Isotherms for the isochoric heat capacity of [bmim][BF_4]. ■, 298.15 K; ▲, 303.15 K; ◆, 308.15 K; □, 313.15 K; △, 318.15 K; ◇, 323.15 K.

At atmospheric pressure, literature data show that whereas Huddleston et al.[17] report 1.12 g·cm^{-3} and 1.17 g·cm^{-3} (their ref 36), values found in the articles of Wang et al.,[24] Seddon et al.,[25] Fredlake et al.,[4] and Tokuda et al.[5] are quoted as 1.21105 g·cm^{-3}, 1.2048 g·cm^{-3}, 1.2037 g·cm^{-3}, and 1.2035 g·cm^{-3}, respectively. (In the latter two cases, a least-squares fit to their data was applied to make comparisons at the same nominal temperature of 298.15 K.)

Table 16. Calculated Values of κ_T for [bmim][BF_4]

	T/K							*T*/K					
p/MPa	298.15	303.15	308.15	313.15	318.15	323.15	*p*/MPa	298.15	303.15	308.15	313.15	318.15	323.15
	κ_T/GPa^{-1}							κ_T/GPa^{-1}					
0.1	0.396_3	0.402_6	0.408_6	0.414_4	0.420_2	0.426_4	70	0.310_6	0.315_0	0.319_2	0.323_2	0.327_0	0.330_6
0.5	0.395_6	0.401_9	0.407_9	0.413_7	0.419_5	0.425_6	75	0.306_0	0.310_4	0.314_5	0.318_4	0.322_1	0.325_7
1	0.394_8	0.401_1	0.407_1	0.412_8	0.418_5	0.424_6	80	0.301_6	0.305_9	0.309_9	0.313_8	0.317_4	0.321_0
3	0.391_6	0.397_8	0.403_7	0.409_3	0.415_0	0.420_9	85	0.297_3	0.301_5	0.305_5	0.309_3	0.312_9	0.316_4
5	0.388_5	0.394_5	0.400_3	0.405_9	0.411_4	0.417_2	90	0.293_2	0.297_3	0.301_2	0.304_9	0.308_5	0.312_0
10	0.380_9	0.386_7	0.392_3	0.397_7	0.403_0	0.408_5	95	0.289_1	0.293_2	0.297_1	0.300_7	0.304_2	0.307_7
15	0.373_6	0.379_3	0.384_7	0.389_9	0.394_9	0.400_1	100	0.285_2	0.289_2	0.293_0	0.296_6	0.300_1	0.303_5
20	0.366_7	0.372_2	0.377_4	0.382_4	0.387_3	0.392_3	105	0.281_4	0.285_4	0.289_1	0.292_7	0.296_1	0.299_4
25	0.360_0	0.365_4	0.370_5	0.375_3	0.380_0	0.384_8	110	0.277_8	0.281_6	0.285_3	0.288_8	0.292_2	0.295_5
30	0.353_6	0.358_9	0.363_8	0.368_6	0.373_1	0.377_6	115	0.274_2	0.278_0	0.281_6	0.285_0	0.288_4	0.291_7
35	0.347_5	0.352_6	0.357_5	0.362_1	0.366_5	0.370_8	120	0.270_7	0.274_4	0.278_0	0.281_4	0.284_6	0.287_9
40	0.341_6	0.346_6	0.351_4	0.355_8	0.360_1	0.364_4	125	0.267_3	0.271_0	0.274_5	0.277_8	0.281_0	0.284_3
45	0.336_0	0.340_9	0.345_5	0.349_9	0.354_1	0.358_1	130	0.264_0	0.267_6	0.271_0	0.274_3	0.277_5	0.280_7
50	0.330_5	0.335_3	0.339_8	0.344_1	0.348_2	0.352_2	135	0.260_8	0.264_4	0.267_7	0.270_9	0.274_1	0.277_3
55	0.325_3	0.330_0	0.334_4	0.338_6	0.342_6	0.346_5	140	0.257_7	0.261_2	0.264_5	0.267_6	0.270_7	0.273_9
60	0.320_2	0.324_8	0.329_2	0.333_3	0.337_2	0.341_0	145	0.254_7	0.258_1	0.261_3	0.264_4	0.267_4	0.270_5
65	0.315_3	0.319_8	0.324_1	0.328_1	0.332_0	0.335_7	150	0.251_7	0.255_0	0.258_2	0.261_2	0.264_2	0.267_3

Table 17. Calculated Values of κ_S for [bmim][BF_4]

	T/K							*T*/K					
p/MPa	298.15	303.15	308.15	313.15	318.15	323.15	*p*/MPa	298.15	303.15	308.15	313.15	318.15	323.15
	κ_S/GPa^{-1}							κ_S/GPa^{-1}					
0.1	0.342_2	0.348_5	0.354_5	0.360_4	0.366_3	0.372_6	70	0.270_0	0.274_1	0.278_0	0.281_7	0.285_3	0.288_8
0.5	0.341_6	0.347_9	0.353_9	0.359_8	0.365_7	0.372_0	75	0.266_1	0.270_2	0.274_0	0.277_6	0.281_1	0.284_5
1	0.340_9	0.347_2	0.353_2	0.359_0	0.364_9	0.371_1	80	0.262_5	0.266_4	0.270_1	0.273_7	0.277_1	0.280_4
3	0.338_2	0.344_4	0.350_3	0.356_0	0.361_8	0.367_9	85	0.258_9	0.262_7	0.266_4	0.269_8	0.273_1	0.276_4
5	0.335_6	0.341_6	0.347_4	0.353_1	0.358_7	0.364_7	90	0.255_4	0.259_2	0.262_7	0.266_1	0.269_4	0.272_5
10	0.329_1	0.335_0	0.340_6	0.346_0	0.351_4	0.357_0	95	0.252_1	0.255_7	0.259_2	0.262_5	0.265_7	0.268_8
15	0.323_0	0.328_6	0.334_0	0.339_2	0.344_4	0.349_7	100	0.248_8	0.252_4	0.255_8	0.259_0	0.262_1	0.265_2
20	0.317_1	0.322_6	0.327_8	0.332_8	0.337_7	0.342_8	105	0.245_6	0.249_1	0.252_5	0.255_6	0.258_7	0.261_7
25	0.311_5	0.316_8	0.321_8	0.326_7	0.331_4	0.336_2	110	0.242_6	0.246_0	0.249_2	0.252_3	0.255_3	0.258_3
30	0.306_1	0.311_2	0.316_1	0.320_8	0.325_4	0.329_9	115	0.239_6	0.242_9	0.246_1	0.249_1	0.252_0	0.254_9
35	0.301_0	0.305_9	0.310_7	0.315_2	0.319_6	0.324_0	120	0.236_7	0.240_0	0.243_0	0.246_0	0.248_8	0.251_7
40	0.296_0	0.300_8	0.305_4	0.309_8	0.314_1	0.318_3	125	0.233_9	0.237_1	0.240_1	0.243_0	0.245_7	0.248_6
45	0.291_2	0.296_0	0.300_4	0.304_7	0.308_8	0.312_8	130	0.231_1	0.234_2	0.237_2	0.240_0	0.242_7	0.245_5
50	0.286_7	0.291_3	0.295_6	0.299_7	0.303_7	0.307_6	135	0.228_4	0.231_5	0.234_3	0.237_1	0.239_8	0.242_5
55	0.282_3	0.286_7	0.291_0	0.295_0	0.298_8	0.302_6	140	0.225_8	0.228_8	0.231_6	0.234_3	0.236_9	0.239_6
60	0.278_0	0.282_4	0.286_5	0.290_4	0.294_2	0.297_8	145	0.223_3	0.226_2	0.228_9	0.231_5	0.234_1	0.236_8
65	0.273_9	0.278_2	0.282_2	0.286_0	0.289_7	0.293_2	150	0.220_8	0.223_6	0.226_3	0.228_8	0.231_3	0.234_0

Table 18. Calculated Values of α_p for [bmim][BF_4]

	T/K							*T*/K					
p/MPa	298.15	303.15	308.15	313.15	318.15	323.15	*p*/MPa	298.15	303.15	308.15	313.15	318.15	323.15
	$10^3\alpha_p$/K^{-1}							$10^3\alpha_p$/K^{-1}					
0.1	0.594_0	0.590_3	0.586_7	0.582_9	0.579_2	0.575_4	70	0.521_5	0.520_3	0.519_1	0.517_9	0.516_6	0.515_4
0.5	0.593_5	0.589_9	0.586_2	0.582_5	0.578_7	0.574_9	75	0.517_1	0.516_1	0.515_0	0.514_0	0.513_0	0.511_9
1	0.592_9	0.589_3	0.585_6	0.581_9	0.578_1	0.574_3	80	0.512_7	0.511_9	0.511_0	0.510_2	0.509_3	0.508_5
3	0.590_5	0.586_9	0.583_2	0.579_6	0.575_8	0.572_1	85	0.508_4	0.507_8	0.507_1	0.506_5	0.505_8	0.505_1
5	0.588_1	0.584_5	0.580_9	0.577_3	0.573_6	0.569_9	90	0.504_2	0.503_7	0.503_2	0.502_8	0.502_3	0.501_8
10	0.582_2	0.578_8	0.575_3	0.571_8	0.568_2	0.564_6	95	0.500_0	0.499_7	0.499_4	0.499_1	0.498_8	0.498_5
15	0.576_5	0.573_2	0.569_9	0.566_5	0.563_1	0.559_6	100	0.496_0	0.495_8	0.495_7	0.495_6	0.495_4	0.495_2
20	0.571_0	0.567_8	0.564_6	0.561_4	0.558_2	0.554_9	105	0.492_0	0.492_0	0.492_0	0.492_0	0.492_0	0.492_0
25	0.565_5	0.562_6	0.559_5	0.556_5	0.553_4	0.550_3	110	0.488_1	0.488_2	0.488_4	0.488_5	0.488_7	0.488_8
30	0.560_2	0.557_4	0.554_6	0.551_8	0.548_9	0.546_0	115	0.484_2	0.484_5	0.484_8	0.485_1	0.485_4	0.485_7
35	0.555_1	0.552_4	0.549_8	0.547_2	0.544_5	0.541_7	120	0.480_5	0.480_9	0.481_3	0.481_7	0.482_1	0.482_6
40	0.550_0	0.547_6	0.545_1	0.542_7	0.540_2	0.537_7	125	0.476_8	0.477_3	0.477_9	0.478_4	0.478_9	0.479_5
45	0.545_0	0.542_8	0.540_6	0.538_3	0.536_0	0.533_7	130	0.473_2	0.473_8	0.474_5	0.475_1	0.475_8	0.476_4
50	0.540_1	0.538_1	0.536_1	0.534_0	0.532_0	0.529_9	135	0.469_6	0.470_4	0.471_1	0.471_9	0.472_6	0.473_4
55	0.535_4	0.533_5	0.531_7	0.529_9	0.528_0	0.526_1	140	0.466_2	0.467_0	0.467_8	0.468_7	0.469_6	0.470_4
60	0.530_7	0.529_1	0.527_4	0.525_8	0.524_1	0.522_5	145	0.462_8	0.463_7	0.464_6	0.465_6	0.466_5	0.467_4
65	0.526_0	0.524_6	0.523_2	0.521_8	0.520_3	0.518_9	150	0.459_5	0.460_5	0.461_5	0.462_5	0.463_5	0.464_5

Our results agree reasonably well with those of Seddon et al., Fredlake et al., and Tokuda et al.

As for α_p, although expansivities decrease sharply with pressure, they decrease mildly as temperature increases. This corroborates previously discussed[23] effects of the anions' size on the temperature coefficient of α_p in which by decreasing the anion's size one finds a tendency for that temperature coefficient to cross over from positive to negative values. In the latter case, the IL should present an "anomaly" (a minimum in the α_p vs *T* plot at some higher temperature[23]). The differences obtained for the derived properties, α_p and κ_T, when comparing the deriva-

Table 19. Calculated Values of γ_v for [bmim][BF_4]

	T/K							*T*/K					
p/MPa	298.15	303.15	308.15	313.15	318.15	323.15	*p*/MPa	298.15	303.15	308.15	313.15	318.15	323.15
	γ_v/MPa·K^{-1}							γ_v/MPa·K^{-1}					
0.1	1.49_9	1.46_6	1.43_6	1.40_7	1.37_8	1.34_9	70	1.67_9	1.65_2	1.62_6	1.60_2	1.58_0	1.55_9
0.5	1.50_0	1.46_8	1.43_7	1.40_8	1.38_0	1.35_1	75	1.69_0	1.66_3	1.63_8	1.61_4	1.59_2	1.57_1
1	1.50_2	1.46_9	1.43_9	1.40_9	1.38_1	1.35_2	80	1.70_0	1.67_3	1.64_9	1.62_6	1.60_5	1.58_4
3	1.50_8	1.47_5	1.44_5	1.41_6	1.38_8	1.35_9	85	1.71_0	1.68_4	1.66_0	1.63_7	1.61_6	1.59_6
5	1.51_4	1.48_1	1.45_1	1.42_2	1.39_4	1.36_6	90	1.72_0	1.69_4	1.67_1	1.64_9	1.62_8	1.60_8
10	1.52_9	1.49_6	1.46_6	1.43_8	1.41_0	1.38_2	95	1.72_9	1.70_4	1.68_1	1.66_0	1.64_0	1.62_0
15	1.54_3	1.51_1	1.48_1	1.45_3	1.42_6	1.39_9	100	1.73_9	1.71_4	1.69_2	1.67_1	1.65_1	1.63_2
20	1.55_7	1.52_6	1.49_6	1.46_8	1.44_1	1.41_5	105	1.74_8	1.72_4	1.70_2	1.68_1	1.66_2	1.64_3
25	1.57_1	1.54_0	1.51_0	1.48_3	1.45_6	1.43_0	110	1.75_7	1.73_4	1.71_2	1.69_2	1.67_3	1.65_4
30	1.58_4	1.55_3	1.52_4	1.49_7	1.47_1	1.44_6	115	1.76_6	1.74_3	1.72_2	1.70_2	1.68_3	1.66_5
35	1.59_7	1.56_7	1.53_8	1.51_1	1.48_6	1.46_1	120	1.77_5	1.75_2	1.73_1	1.71_2	1.69_4	1.67_6
40	1.61_0	1.58_0	1.55_2	1.52_5	1.50_0	1.47_6	125	1.78_3	1.76_1	1.74_1	1.72_2	1.70_4	1.68_7
45	1.62_2	1.59_2	1.56_5	1.53_9	1.51_4	1.49_0	130	1.79_2	1.77_0	1.75_0	1.73_2	1.71_4	1.69_7
50	1.63_4	1.60_5	1.57_8	1.55_2	1.52_8	1.50_4	135	1.80_1	1.77_9	1.76_0	1.74_2	1.72_5	1.70_7
55	1.64_6	1.61_7	1.59_0	1.56_5	1.54_1	1.51_8	140	1.80_9	1.78_8	1.76_9	1.75_1	1.73_5	1.71_8
60	1.65_7	1.62_9	1.60_2	1.57_8	1.55_4	1.53_2	145	1.81_7	1.79_7	1.77_8	1.76_1	1.74_5	1.72_8
65	1.66_8	1.64_0	1.61_4	1.59_0	1.56_7	1.54_6	150	1.82_5	1.80_6	1.78_7	1.77_1	1.75_4	1.73_8

Table 20. Calculated Values of C_p for [bmim][BF_4]

	T/K							*T*/K					
p/MPa	298.15	303.15	308.15	313.15	318.15	323.15	*p*/MPa	298.15	303.15	308.15	313.15	318.15	323.15
	C_p/kJ·K^{-1}kg^{-1}							C_p/kJ·K^{-1}kg^{-1}					
0.1	1.61_3	1.62_5	1.63_7	1.65_0	1.66_3	1.67_7	70	1.61_7	1.62_8	1.64_1	1.65_4	1.66_7	1.68_1
0.5	1.61_3	1.62_5	1.63_7	1.65_0	1.66_3	1.67_7	75	1.61_7	1.62_8	1.64_1	1.65_4	1.66_7	1.68_1
1	1.61_4	1.62_5	1.63_7	1.65_0	1.66_3	1.67_7	80	1.61_7	1.62_8	1.64_1	1.65_4	1.66_7	1.68_1
3	1.61_4	1.62_5	1.63_7	1.65_0	1.66_3	1.67_7	85	1.61_7	1.62_8	1.64_0	1.65_3	1.66_7	1.68_1
5	1.61_4	1.62_5	1.63_7	1.65_0	1.66_4	1.67_7	90	1.61_6	1.62_8	1.64_0	1.65_3	1.66_7	1.68_1
10	1.61_4	1.62_6	1.63_8	1.65_1	1.66_4	1.67_8	95	1.61_6	1.62_8	1.64_0	1.65_3	1.66_7	1.68_1
15	1.61_5	1.62_6	1.63_8	1.65_1	1.66_5	1.67_9	100	1.61_6	1.62_8	1.64_0	1.65_3	1.66_6	1.68_0
20	1.61_5	1.62_7	1.63_9	1.65_2	1.66_5	1.67_9	105	1.61_6	1.62_7	1.64_0	1.65_2	1.66_6	1.68_0
25	1.61_5	1.62_7	1.63_9	1.65_2	1.66_5	1.67_9	110	1.61_5	1.62_7	1.63_9	1.65_2	1.66_6	1.68_0
30	1.61_6	1.62_7	1.64_0	1.65_2	1.66_6	1.68_0	115	1.61_5	1.62_7	1.63_9	1.65_2	1.66_5	1.67_9
35	1.61_6	1.62_8	1.64_0	1.65_3	1.66_6	1.68_0	120	1.61_5	1.62_6	1.63_9	1.65_1	1.66_5	1.67_9
40	1.61_6	1.62_8	1.64_0	1.65_3	1.66_6	1.68_1	125	1.61_4	1.62_6	1.63_8	1.65_1	1.66_4	1.67_9
45	1.61_7	1.62_8	1.64_0	1.65_3	1.66_7	1.68_1	130	1.61_4	1.62_5	1.63_8	1.65_1	1.66_4	1.67_8
50	1.61_7	1.62_8	1.64_1	1.65_3	1.66_7	1.68_1	135	1.61_3	1.62_5	1.63_7	1.65_0	1.66_4	1.67_8
55	1.61_7	1.62_8	1.64_1	1.65_4	1.66_7	1.68_1	140	1.61_3	1.62_5	1.63_7	1.65_0	1.66_3	1.67_7
60	1.61_7	1.62_8	1.64_1	1.65_4	1.66_7	1.68_1	145	1.61_2	1.62_4	1.63_6	1.64_9	1.66_3	1.67_7
65	1.61_7	1.62_9	1.64_1	1.65_4	1.66_7	1.68_1	150	1.61_2	1.62_4	1.63_6	1.64_9	1.66_2	1.67_6

Table 21. Calculated Values of C_v for [bmim][BF_4]

	T/K							*T*/K					
p/MPa	298.15	303.15	308.15	313.15	318.15	323.15	*p*/MPa	298.15	303.15	308.15	313.15	318.15	323.15
	C_v/kJ·K^{-1}·kg^{-1}							C_v/kJ·K^{-1}·kg^{-1}					
0.1	1.39_3	1.40_6	1.42_0	1.43_5	1.45_0	1.46_6	70	1.40_5	1.41_7	1.42_9	1.44_2	1.45_5	1.46_8
0.5	1.39_3	1.40_7	1.42_0	1.43_5	1.45_0	1.46_6	75	1.40_6	1.41_8	1.42_9	1.44_2	1.45_5	1.46_8
1	1.39_3	1.40_7	1.42_0	1.43_5	1.45_0	1.46_6	80	1.40_7	1.41_8	1.43_0	1.44_2	1.45_5	1.46_8
3	1.39_4	1.40_7	1.42_1	1.43_5	1.45_0	1.46_6	85	1.40_8	1.41_9	1.43_0	1.44_2	1.45_5	1.46_8
5	1.39_4	1.40_7	1.42_1	1.43_5	1.45_0	1.46_6	90	1.40_8	1.41_9	1.43_1	1.44_3	1.45_5	1.46_8
10	1.39_5	1.40_8	1.42_2	1.43_6	1.45_1	1.46_7	95	1.40_9	1.42_0	1.43_1	1.44_3	1.45_5	1.46_8
15	1.39_6	1.40_9	1.42_3	1.43_7	1.45_1	1.46_7	100	1.41_0	1.42_0	1.43_1	1.44_3	1.45_5	1.46_8
20	1.39_7	1.41_0	1.42_3	1.43_7	1.45_2	1.46_7	105	1.41_0	1.42_1	1.43_2	1.44_3	1.45_5	1.46_8
25	1.39_8	1.41_1	1.42_4	1.43_8	1.45_2	1.46_7	110	1.41_1	1.42_1	1.43_2	1.44_3	1.45_5	1.46_8
30	1.39_9	1.41_1	1.42_5	1.43_8	1.45_3	1.46_8	115	1.41_1	1.42_2	1.43_2	1.44_4	1.45_6	1.46_8
35	1.40_0	1.41_2	1.42_5	1.43_9	1.45_3	1.46_8	120	1.41_2	1.42_2	1.43_3	1.44_4	1.45_6	1.46_8
40	1.40_0	1.41_3	1.42_6	1.43_9	1.45_3	1.46_8	125	1.41_2	1.42_2	1.43_3	1.44_4	1.45_6	1.46_8
45	1.40_1	1.41_4	1.42_6	1.44_0	1.45_4	1.46_8	130	1.41_3	1.42_3	1.43_3	1.44_4	1.45_6	1.46_8
50	1.40_2	1.41_4	1.42_7	1.44_0	1.45_4	1.46_8	135	1.41_3	1.42_3	1.43_3	1.44_4	1.45_5	1.46_8
55	1.40_3	1.41_5	1.42_8	1.44_1	1.45_4	1.46_8	140	1.41_3	1.42_3	1.43_3	1.44_4	1.45_5	1.46_7
60	1.40_4	1.41_6	1.42_8	1.44_1	1.45_4	1.46_8	145	1.41_4	1.42_3	1.43_3	1.44_4	1.45_5	1.46_7
65	1.40_5	1.41_6	1.42_9	1.44_1	1.45_5	1.46_8	150	1.41_4	1.42_4	1.43_4	1.44_4	1.45_5	1.46_7

tion of the measured densities with the integration method show average deviations of 4% and −4%, respectively. Although these values are within acceptable limits, they corroborate the strong dependence of the derivation method on the shape of the curves used to fit the experimental data and the necessity of collecting a large number of experimental points.

As for the heat capacities, the results for both the isobaric and isochoric heat capacities reveal, in practice, pressure independence.

Conclusions

This work shows the usefulness of this method in deriving precise thermodynamic properties at high pres-

sures from speed of sound measurements. It maps the physical behavior of two important ionic liquids over wide pressure and temperature ranges.

As the anion increases in size ($[BF_4]^- < [PF_6]^-$), the density increases accordingly, whereas the speed of sound shows the opposite trend. At first glance, this fact may seem counterintuitive because one tends to associate greater density with greater speed of sound. This line of thought mainly arises from comparisons (in density and speed of sound) made between the gas phase and the condensed phase. It is true that gases present smaller densities as well as speeds of propagation of sound waves than condensed phases, but this truism has little to do with density. The typical ratio between the densities of liquid to gas (far from the critical point) is on the order of thousands. However, the ratio (gas to liquid) of compressibilities is ca. 100 000. Therefore, compressibility is the factor that controls the speed of sound. It is also interesting that in these ILs (differing in the anion) if the mass density increases the molar volume also does. For instance, at atmospheric pressure and 298.15 K $V_{\mathrm{bmimPF_6}} - V_{\mathrm{bmimBF_4}} = 20.3\ \mathrm{cm^3 \cdot mol^{-1}}$. This value can be attributed to the increase in the effective anion size[3] from 0.089 $\mathrm{nm^3}$/anion of BF_4^- to 0.122 $\mathrm{nm^3}$/anion of PF_6^-.

Generally, one can state that speed of sound values of ILs are not too dissimilar from those typically found in conventional solvents, tending to fall in the high-value side of the range. In contrast, both compressibilities and expansivities are ca. three times smaller than values typically found in those conventional solvents. This is probably a consequence of the fact that although critical temperatures, T_c, are unknown for ILs, estimates of T_c of ILs[26] show that their critical temperatures are certainly much higher (if it were possible to reach the liquid−gas critical point by avoiding the thermal decomposition of the IL) than those of molecular solvents. Therefore, in the case of ILs, room-temperature conditions certainly correspond to very low reduced temperatures. It is well known that both compressibility and expansivity decrease drastically along the orthobaric line from an infinite value at the critical point to very modest values as temperature (and reduced temperature) decreases.

As for heat capacities, if comparisons are performed using molar quantities, for instance, at atmospheric pressure and 298.15 K, then $C_{p,\mathrm{bmimPF_6}} - C_{p,\mathrm{bmimBF_4}} = 44.1\ \mathrm{J \cdot mol^{-1} \cdot K^{-1}}$. The greater values presented by PF_6^- are mainly a consequence of the larger number of vibrational degrees of freedom of this anion compared with that of BF_4^-. In other words, as the anion's structural complexity increases, one expects improved energy storage ability.

Acknowledgment

We thank the QUILL group, Belfast, lead by Professor Kenneth Seddon for hosting some of us and helping with the synthesis and purification of [bmim][PF_6].

Literature Cited

(1) (a) Visser, A. E.; Swatloski, R. P.; Reichert, W. M.; Griffin, S. T.; Rogers, R. D. Traditional Extractants in Nontraditional Solvents: Groups 1 and 2 Extraction by Crown Ethers in Room-Temperature Ionic Liquids. *Ind. Eng. Chem. Res.* **2000**, *39*, 3596−3604. (b) Swatloski, R. P.; Holbrey, J. D.; Rogers, R. D. Ionic liquids are not always green: hydrolysis of 1-butyl-3-methylimidazolium hexafluorophosphate. *Green Chem.* **2003**, *5*, 361−363.

(2) Najdanovic-Visak, V.; Esperança, J. M. S. S.; Rebelo, L. P. N.; Nunes da Ponte, M.; Guedes, H. J. R.; Seddon, K. R.; Szydlowski, J. Phase behaviour of room temperature ionic liquid solutions: an unusually large co-solvent effect in (water + ethanol). *Phys. Chem. Chem. Phys.* **2002**, *4*, 1701−1703.

(3) Rebelo, L. P. N.; Najdanovic-Visak, V.; Gomes de Azevedo, R.; Esperança, J. M. S. S.; Nunes da Ponte, M.; Guedes, H. J. R.; Visak, Z. P.; de Sousa, H. C.; Szydlowski, J.; Canongia Lopes, J. N.; Cordeiro, T. C. Phase Behavior and Thermodynamic Properties of Ionic Liquids, Ionic Liquid Mixtures, and Ionic Liquid Solutions. In *Ionic Liquids IIIA: Fundamentals, Progress, Challenges, and Opportunities−Properties and Structure*; Rogers, R., Seddon, K. R., Eds.; ACS Symposium Series 901; American Chemical Society: Washington DC, 2005; Chapter 21, 260−281.

(4) Fredlake, C. P.; Crosthwaite, J. M.; Hert, D. G.; Aki, S. N. V. K.; Brennecke, J. F. Thermophysical Properties of Imidazolium-Based Ionic Liquids. *J. Chem. Eng. Data*. **2004**, *49*, 954−964.

(5) Tokuda, H.; Hayamizu, K.; Ishii, K.; Susan, M. A. B. H.; Watanabe, M. Physicochemical Properties and Structures of Room-Temperature Ionic Liquids. 1. Variation of Anionic Species. *J. Phys. Chem. B* **2004**, *108*, 16593−16600.

(6) Marsh, K. N.; Boxall, J. A.; Lichtenthaler, R. Room-Temperature Ionic Liquids and Their Mixtures − a Review. *Fluid Phase Equilib.* **2004**, *219*, 93−98.

(7) Gomes de Azevedo, R.; Szydlowski, J.; Pires, P. F.; Esperança, J. M. S. S.; Guedes, H. J. R.; Rebelo, L. P. N. A novel nonintrusive microcell for sound-speed measurements in liquids. Speed of sound and thermodynamic properties of 2-propanone at pressures up to 160 MPa. *J. Chem. Thermodyn.* **2004**, *36*, 211−222.

(8) Szydlowski, J.; Gomes de Azevedo, R.; Rebelo, L. P. N.; Esperança, J. M. S. S.; Guedes, H. J. R. Deuterium isotope differences in 2-propanone, $(CH_3)_2CO/(CD_3)_2CO$: a high-pressure sound-speed, density, and heat capacities study. *J. Chem. Thermodyn.* **2005**, *37*, in press (doi: 10.1016/j.jct.2004.11.001).

(9) Trusler, J. P. M. *Physical Acoustics and Metrology of Fluids*; Adam Hilger: Bristol, U.K., 1991.

(10) Douhéret, G.; Davis, M. I.; Reis, J. C. R.; Blandamer, M. J. Isentropic Compressibilities-Experimental Origin and the Quest for their Rigorous Estimation in Thermodynamically Ideal Liquid Mixtures. *Chem. Phys. Chem.* **2001**, *2*, 148−161.

(11) Pires, P. F.; Esperança, J. M. S. S.; Guedes, H. J. R. Ultrasonic Speed of Sound and Derived Thermodynamic Properties of Liquid 1,1,1,2,3,3,3-Heptafluoopropane (HFC227ea) from 248 K to 333 K and Pressures up to 65 MPa. *J. Chem. Eng. Data* **2000**, *45*, 496−502.

(12) Daridon, J. L.; Lagrabette, A.; Lagourette, B. Speed of sound, density, and compressibilities of heavy synthetic cuts from ultrasonic measurements under pressure. *J. Chem. Thermodyn.* **1998**, *30*, 607−623.

(13) (a) Private communication, Kenneth N. Marsh: Lundstrum, R.; Goodwin, A. R. H.; Hsu, K.; Frels, M.; Caudwell, D. R.; Trusler, J. P. M.; Marsh, K. N. Measurement of the Viscosity and Density of Two Reference Fluids, with Nominal Viscosity at $T = 298$ K and $p = 0.1$ Mpa of (16 and 29) mPa·s, at Temperatures between (298 and 398) K and Pressures below 55 Mpa *J. Chem. Eng. Data* 2005, submitted for publication. (b) Fitzgerald, D. *Technical Assessment of the Anton Paar DMA5000 Density Meter*; H & D Fitzgerald Ltd. Publishers, 2000 (http://www.density.co.uk/review_of_5000.pdf).

(14) Gordon, C. M.; Holbrey, J. D.; Kennedy, R.; Seddon, K. R. Ionic Liquid Crystals: Hexafluorophosphate Salts. *J. Mater. Chem.* **1998**, *8*, 2627−2636.

(15) Bonhôte, P.; Dias. A.-P.; Armand, M.; Papageorgiou, N.; Kalyanasundaram, K.; Gratzel, M. Hydrophobic, Highly Conductive Ambient-Temperature Molten Salts. *Inorg. Chem.* **1996**, *35*, 1168−1178.

(16) Debenedetti, P. G. *Metastable Liquids*; Princeton University Press: Princeton, NJ, 1996.

(17) Huddleston, J. G.; Visser, A. E.; Reichert, W. M.; Willauer, H. D.; Broker, G. A.; Rogers, R. D. Characterization and comparison of hydrophilic and hydrophobic room-temperature ionic liquids incorporating the imidazolium cation. *Green Chem.* **2001**, *3*, 156−164.

(18) Kabo, G. J.; Blokhin, A. V.; Paulechka, Y. U.; Kabo, A. G.; Shymanovich, M. P.; Magee, J. W. Thermodynamic Properties of 1-Butyl-3-methylimidazolium Hexafluorophosphate in the Condensed State. *J. Chem. Eng. Data* **2004**, *49*, 453−461.

(19) Domanska, U.; Marciniak, A. Solubility of 1-Alkyl-3-methylimidazolium Hexafluorophosphate in Hydrocarbons. *J. Chem. Eng. Data* **2003**, *48*, 451−456.

(20) Gu, Z.; Brennecke, J. F. Volume Expansivities and Isothermal Compressibilities of Imidazolium and Pyridinium-Based Ionic Liquids. *J. Chem. Eng. Data* **2002**, *47*, 339−345.

(21) Canongia Lopes, J. N.; Cordeiro, T. C.; Esperança, J. M. S. S.; Guedes, H. J. R.; Huk, S.; Rebelo, L. P. N.; Seddon, K. R. Deviations from Ideality in Mixtures of Two Ionic Liquids Containing a Common Ion. *J. Phys. Chem. B* **2005**, *109*, 3519−3525.

(22) Sun, T.; Biswas, S. N.; Trappeniers, N. J.; Seldam, C. A. T. Acoustic and Thermodynamic Properties of Methanol from 273 to 333 K and at Pressures to 280 MPa. *J. Chem. Eng. Data* **1988**, *33*, 395−398.

(23) Rebelo, L. P. N.; Najdanovic-Visak, V.; Visak Z. P.; Nunes da Ponte, M.; Szydlowski, J.; Cerdeiriña, C. A.; Troncoso, J.; Romani, L.; Esperança, J. M. S. S.; Guedes, H. J. R.; de Sousa, H. C. A detailed thermodynamic analysis of $[C_4mim][BF_4]$ + Water as a case study to model ionic liquid aqueous solutions. *Green Chem.* **2004**, *6*, 369−381.
(24) Wang, J.; Tian, Y.; Zhao, Y.; Zhuo, K. A volumetric and viscosity study for the mixtures of 1-n-butyl-3-methylimidazolium tetrafluoroborate ionic liquid with acetonitrile, dichloromethane, 2-butanone and N, N − dimethylformamide. *Green Chem.* **2003**, *5*, 618−622.
(25) Seddon, K. R.; Stark, A.; Torres, M.−J. Viscosity and density of 1-alkyl-3-methylimidazolium ionic liquids. In *Clean Solvents: Alternative Media for Chemical Reactions and Processing*; Abraham, M., Moens, L., Eds.; ACS Symposium Series 819; American Chemical Society: Washington, DC, 2002; pp 34−49.
(26) Rebelo, L. P. N.; Canongia Lopes, J. N.; Esperança, J. M. S. S.; Filipe, E. On the Critical Temperature, Normal Boiling Point, and Vapor Pressure of Ionic Liquids. *J. Phys. Chem. B* **2005**, *109*, 6040−6043.

Received for review December 29, 2004. Accepted March 23, 2005. This work was financially supported by Fundação para a Ciência e Tecnologia, Portugal, under contract POCTI/EQU/35437/00. R.G.A., J.M.S.S.E., V.N.-V. and Z.P.V. are grateful to Fundação para a Ciência e Tecnologia for doctoral fellowships.

JE049534W